Exploring Structural Diversity and Fluxionality of Pt$_n$ (n = 10−13) Clusters from First-Principles

Victor Fung and De-en Jiang*[ID]

Department of Chemistry, University of California, Riverside, California 92521, United States

S *Supporting Information*

ABSTRACT: Subnanometer transition-metal clusters have been shown to possess catalytic activity that is size-dependent. It has been suggested that the fluxionality of these small clusters may be closely related to their catalytic activity. Here we use basin-hopping global optimization with density functional theory (DFT) to study the energy landscape of Pt$_n$ (n = 10−13) clusters. We analyze a large set of local minima obtained from the DFT-based global optimization. We find that Pt$_{10}$ is unique with respect to the other studied sizes in its structural landscape, which shows a single, distinct structural motif corresponding to a tetrahedral global minimum. In contrast, Pt$_{11−13}$ all display characteristics of high fluxionality with the presence of multiple significantly differing structural features in the low-energy region, as characterized by coordination number, interatomic distances, and shape. These observations demonstrate the structural diversity and fluxionality of the subnanometer Pt clusters that will have important implications for catalysis.
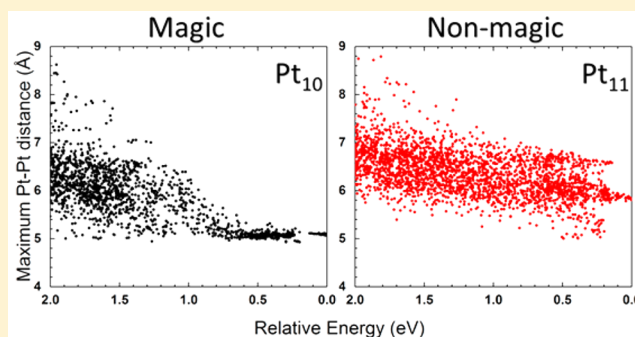
1. INTRODUCTION

Subnanometer transition-metal clusters are of considerable research interest in chemistry. These clusters often possess electronic, magnetic, and catalytic properties very different from those of the bulk. In particular, platinum surfaces and clusters are an industrially important catalyst for a wide variety of reactions, from electrochemistry such as hydrogen evolution reaction (HER) and oxygen reduction reaction (ORR)[1−4] to catalytic activation of alkanes.[5] A recent shift from Pt surfaces to nanosystems focuses on 5−30 atoms, which show significantly increased activity.[1,4−10]

For clusters in this size regime, small changes in the coordination and morphology can have a significant impact on properties such as molecular adsorption.[11,12] It is therefore necessary to explore the energy landscape of these small-sized clusters. Structure prediction through global optimization is one such method to obtain the global minimum structures through theoretical modeling. Many examples of global optimization algorithms exist in use today, including genetic algorithms, particle swarm optimization, and basin hopping.[13−15]

The key to the global optimization scheme is the method to evaluate energy and forces of the sampled structures for geometry optimization. Because global optimization needs to sample a significant number of possible structures, the evaluation of cluster energy can be expensive. While semi-empirical potentials are a popular and relatively inexpensive method, they are, in general, not accurate enough to describe the energy landscape of transition-metal nanoclusters. This necessitates the use of a more accurate method such as density functional theory (DFT).

Small Pt clusters of size 10−13 sit near the peak of catalytic activity for some reactions[5,8,9,16] and are of special interest because they are more amenable to DFT-based global minimization than the larger sizes. While locating stable Pt clusters in this size regime has been pursued before,[17−19] a detailed analysis of the structure diversity and its correlation with the energy has not been demonstrated. Herein we will use DFT local minimization with basin hopping to explore the energy landscape of Pt subnanometer clusters. More importantly, we will take advantage of the large number of local minima obtained to investigate structure−energy relationships for these Pt clusters, thereby giving us a more fundamental understanding of their properties than the global minima alone.

2. METHODS

First-principles local optimization with DFT is used in conjunction with the global minimum search using basin hopping (BH).[20] The general scheme of basin-hopping global minimum search for clusters has been described by Wales et al. with Lennard-Jones potentials[15] and later applied using first-

principles methods such as DFT for a variety of transition metals.[13,14] Basin hopping is a Monte Carlo method that transforms the potential-energy landscape into steps of local minima: Starting with an initial local minimum (E_0), all atoms are randomly displaced off their equilibrium positions and then the structure is locally optimized (E_1). A Metropolis sampling is then performed: The new structure is accepted when a randomly generated number, n, between 0 and 1 is less than the Boltzmann factor, $e^{-\Delta E/kT}$, where T is an artificial temperature to control the importance of $\Delta E = E_1 - E_0$. Then, the sequence of random move, local minimization, and Metropolis sampling is repeated. In this work, the BH algorithm was used at a temperature of 7500 K for the Metropolis sampling, and the step size of random moves was dynamically updated to maintain an acceptance ratio of 50%. A total of around 20 000 Monte Carlo (MC) steps were performed, including five long parallel runs of 1000 steps each using different starting configurations for each cluster size. For each MC step, the optimized configurations were then analyzed by calculating a variety of its structural properties.

The local optimization at each Monte Carlo step was interfaced with the Vienna Ab Initio Simulation Package (VASP)[21,22] using DFT in a cubic cell of 18 Å on each side. The Perdew−Burke−Erznerhof (PBE)[23] form of the generalized-gradient approximation (GGA) was chosen for electron exchange and correlation. The electron−core interaction was described using the projector-augmented wave method (PAW).[24,25] The Brillouin zone was sampled using the Γ point only. All calculations in this work were performed with spin polarization. After the putative global minimum was found, accurate calculations were performed using a higher energy cutoff of 400 eV for optimizations.

The binding energy of a cluster is calculated with the formula $E_b(n) = [E(Pt_n) - nE(Pt_1)]/n$, where $E(Pt_n)$ is the energy of the cluster and $E(Pt_1)$ is the energy of the isolated Pt atom. Using DFT-PBE, we found the E_b of the Pt−Pt dimer to be −1.86 eV and the Pt−Pt distance to be 2.33 Å, in good agreement with previous theoretical[18,26] and experimental[27] works. Prolateness/oblateness parameter η is obtained from the formula $\eta = (2I_b - I_a - I_c)/I_a$, where $I_a \geq I_b \geq I_c$ are the principal moments of inertia obtained by diagonalizing the moment of inertia tensor in Cartesian coordinates.[28] A negative value corresponds to an oblate spheroid, and a positive value corresponds to a prolate spheroid; in a perfect sphere, $\eta = 0$. The variance of the cluster is simply $\sigma^2 = \Sigma(x_i - x_{com})^2/n$, where x_i is the coordinate of the ith atom in the cluster and x_{com} is the position of the center of mass.

3. RESULTS AND DISCUSSION

Basin-Hopping Global Optimization of Pt Clusters. Figure 1 shows an example of a DFT-BH run for Pt_{13}, starting from an icosahedral initial structure (Figure 1a) obtained from the Cambridge cluster database.[29] The global minimum (Figure 1b) was found surprisingly quickly in this particular run in only 20 steps, despite the structural difference between the initial and the global optimum. Other low-lying isomers are also displayed, including one at step 717 (Figure 1c) and one at step 803 (Figure 1d).

Similar DFT-BH runs were performed for all clusters from Pt_{10} to Pt_{13}, with each cluster size containing around 5000 Monte Carlo steps. In all of the cluster sizes, the global minimum was found in at least two separate parallel DFT-BH runs starting from different initial configurations. The structures
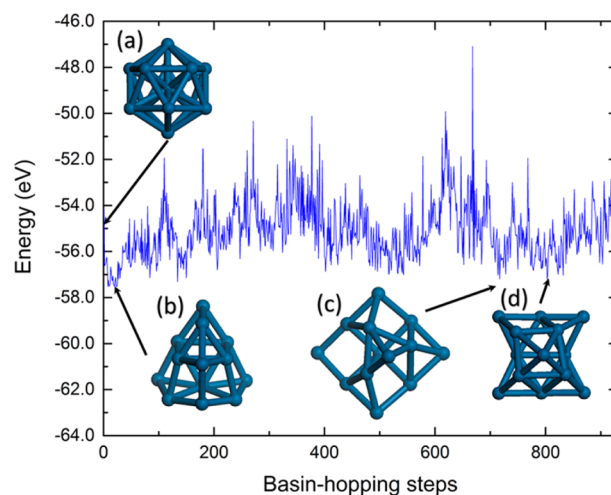
Figure 1. DFT basin-hopping run for Pt_{13}. The Pt_{13} icosahedron (a) was used as the starting structure for this example, and the global minimum was found in structure (b). Other low-energy structures in this run (c and d) are also shown.

of the putative global minima are shown in Figure 2. One can see that Pt_{10} has the highest symmetry with a tetrahedral
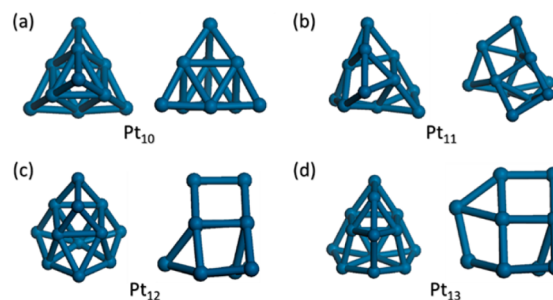
Figure 2. Putative global minima from DFT basin-hopping runs: (a) Pt_{10}, (b) Pt_{11}, (c) Pt_{12}, and (d) Pt_{13}. Two different views are shown for each structure.

geometry, and Pt_{11} has the lowest symmetry. Pt_{12} and Pt_{13} have similar geometry, with Pt_{13} having an additional atom attached to the side of the Pt_{12} structure. The features of these putative global minima are compared in Table 1.

It is evident that Pt_{10} is unique and can be considered a "magic cluster" given its high symmetry. This structure has been previously found by both semiempirical methods and other means of global optimization.[18,19] Furthermore, experimentally, it has been suggested that Pt_{10} is a magic cluster[19,30] with a significantly lower reactivity[30−32] than other clusters in this size regime. Meanwhile, we did not find any evidence that the $n = 11$−13 sizes contained magic clusters. The putative global minimum structure for Pt_{13} was significantly lower in energy than the icosahedral geometry and is in agreement with a recent structure search[26] that found the same global minimum structure in comparison with previously examined structural models.[26,33−35] The same global minimum was also found for Pt_{12}.[26] Including spin−orbit coupling was found to have a minor impact (~0.01 eV) on the relative energy between low-energy structures,[26,36] so we did not consider it in the present work. The putative global minimum for Pt_{11} as a highly disordered geometry (Figure 2b) is, however, dissimilar from other proposed structures in the literature.[18,19]

Table 1. Binding Energy (E_b), Minimum Pt−Pt Distance (min. Pt−Pt), Maximum Pt−Pt Distance (max. Pt−Pt), Average Coordination Number (avg. C.N.; Pt−Pt distance cutoff at 2.900 Å), Oblateness/Prolateness (O/P), and Magnetic Moment (mag. mom.) of the Global Minima of Pt$_n$ (n = 10−13)

cluster size	E_b (eV)	min. Pt−Pt (Å)	max. Pt−Pt (Å)	avg. C.N.	O/P	mag. mom. (μ_B)
10	−3.70	2.534	5.08	4.80	−0.0020	8
11	−3.71	2.509	5.81	3.82	0.0931	2
12	−3.76	2.506	5.77	4.17	0.1028	2
13	−3.83	2.509	6.10	4.15	−0.0478	2
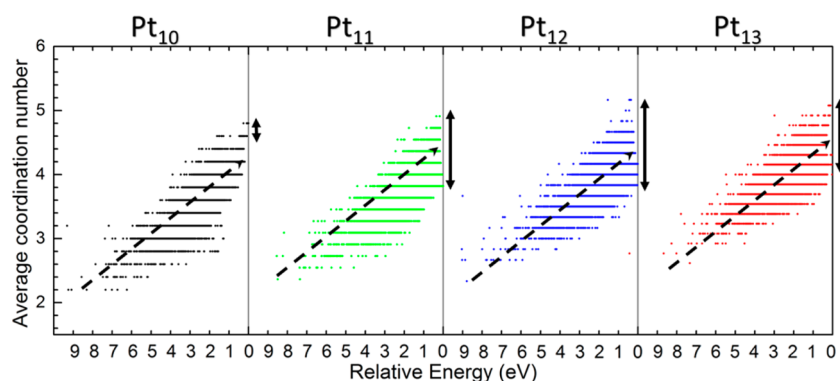
Figure 3. Average coordination number versus energy for all local minima from the DFT basin-hopping run for each cluster size. The vertical line at zero relative energy on the right side of each panel denotes the lowest energy structure. Each dot represents a local minimum.
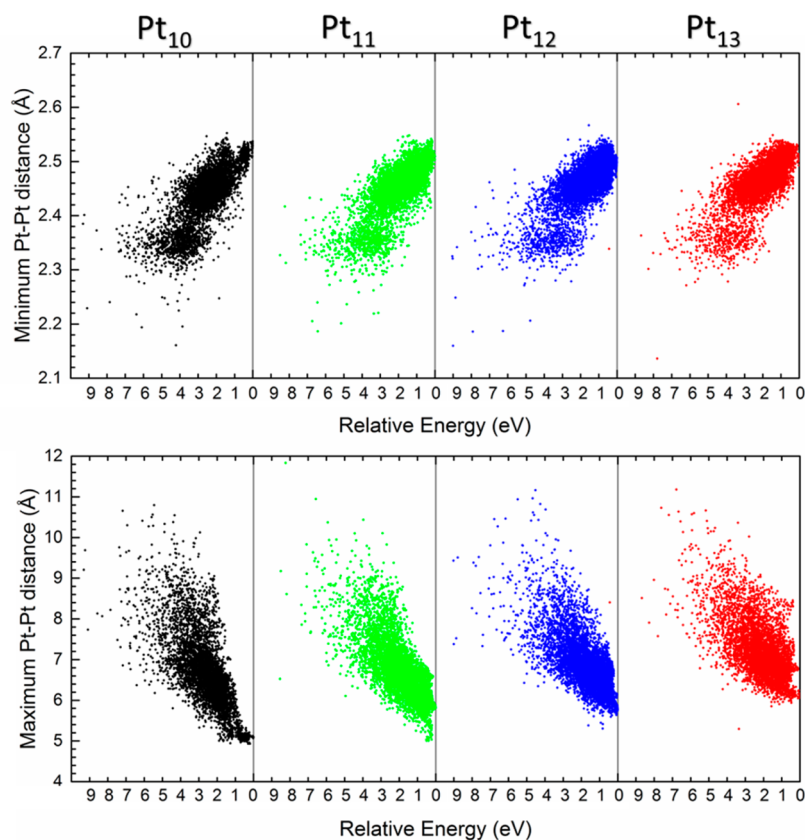
Figure 4. Upper panel: Minimum Pt−Pt distance versus energy for all local minima of Pt$_n$ (n = 10−14) from the DFT basin-hopping runs. Lower panel: Maximum Pt−Pt distance versus energy for all local minima of Pt$_n$ (n = 10−14) the DFT basin-hopping runs. Each dot represents a local minimum.

Coordination-Energy Correlation. Although the global minima are important, it is equally interesting to examine the structure diversity of the isomers, especially those whose energies are close to that of the global minimum. To analyze these structures, we first examined the coordination-energy correlation of the Pt clusters by looking at the average coordination number (that is, averaging the coordination numbers of all atoms in a cluster structure with a cutoff
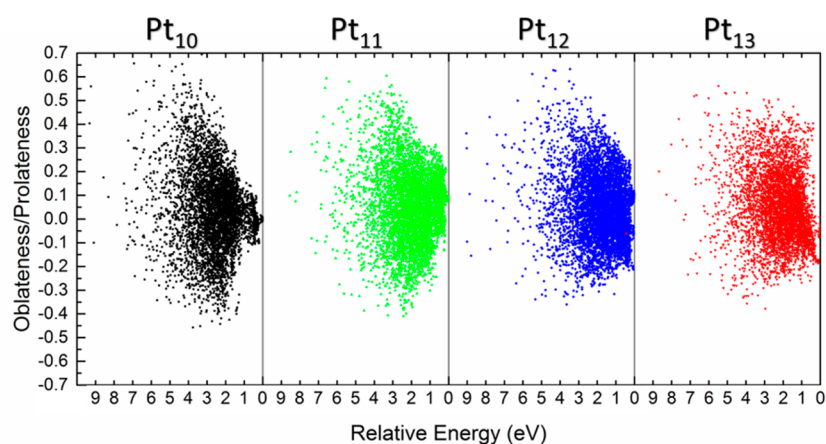
Figure 5. Oblateness/prolateness (O/P or η) versus energy for all local minima of Pt_n ($n = 10-14$) from the DFT basin-hopping runs. Positive η, oblate; negative η, prolate; $\eta = 0$, spherical like. The vertical line at zero relative energy on the right side of each panel denotes the lowest energy structures. Each dot represents a local minimum.
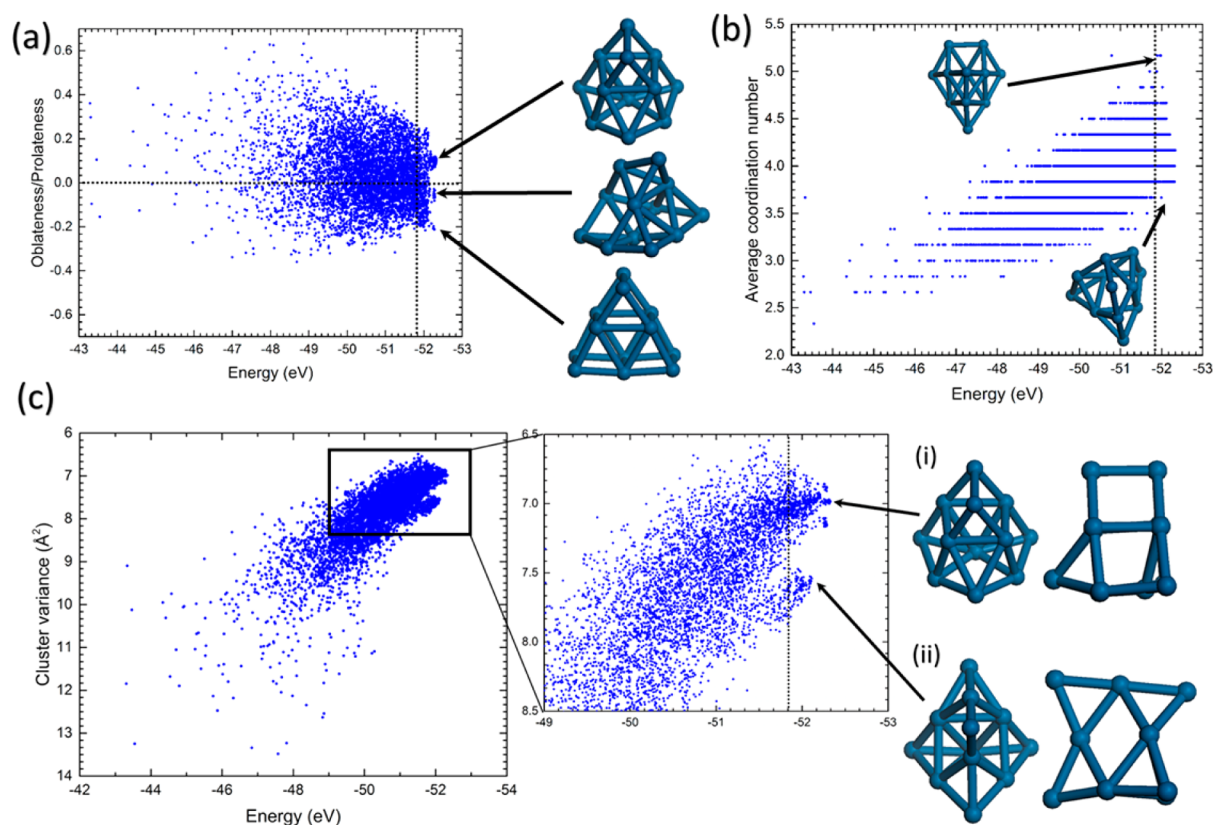
Figure 6. In-depth look of the structural fluxionality of Pt_{12}: (a) oblateness/prolateness (O/P) versus energy, (b) average coordination number versus energy, and (c) cluster variance versus energy. The dashed vertical lines separate clusters within 0.5 eV from the global minimum. Each dot represents a local minimum.

distance of 2.900 Å) for all of the isomers explored along the DFT-BH steps. One would expect that a cluster with a higher average coordination number to be more stable due to the greater number of stabilizing Pt–Pt interactions that would lower the energy of the cluster.

Figure 3 shows that there is a clear trend of decreasing energy or increasing stability with coordination, especially for $n = 10$, suggesting that a higher coordination number indeed corresponds to more stable structures. However, when reaching the low-energy region (right side of each panel in Figure 3), there is also a significant spread in the average coordination of

up to one for the $n = 11-13$ cases. In fact, the structure with the highest average coordination number is not necessarily the lowest energy structure. For example, while the highest average coordination number of the structures in the low-energy region can reach over 5, the average coordination number of the lowest energy structures with the exception of $n = 10$ is much lower than that (4.15 to 4.18 for $n = 11-13$). This result has two important implications. First, it clearly shows that there is a general trend where a higher coordination number roughly corresponds to a lower energy structure, especially for Pt_{10}, whose global minimum is highly symmetric and can be

considered a magic cluster. Second, for clusters whose global minima are less symmetric (for example, $n = 11-13$ in this study), low-lying isomers near the global minimum can be very different in structure given their large variation in the average coordination number. We will see further evidence of the fluxionality of these clusters in the following sections.

Distance−Energy Correlation. Whereas coordination contains some chemical property by only selecting interactions that are within a bonding range, interatomic distances are a more geometric and fundamental parameter of a cluster. Figure 4 shows how Pt−Pt distance and energy are correlated. We find a rough correlation between higher minimum (or nearest neighbor) Pt−Pt distance and lower energy, where the distance increases toward the bulk value. We also find a correlation between lower maximum Pt−Pt distance and lower energy. So, low-energy structures tend to have geometries with high minimum Pt−Pt distance and low maximum Pt−Pt distance. The intuitive reasons behind this trend can be explained as follows. Clusters with a high minimum Pt−Pt distance tend to also have high coordination, as the Pt−Pt bond elongates from a Pt−Pt dimer with a single bond of ∼2.3 Å to the bulk length of 2.8 Å. Thus it should follow that clusters with properties closer to the bulk should have a lower energy, with the bulk energy being the lowest. Meanwhile, clusters with a low maximum interatomic distance tend to describe more compact and better coordinated clusters, which should also be lower in energy than more diffuse and disorganized clusters.

Examining the low-lying structures (those close to the zero-energy line on the right of each panel in Figure 4), we found that the fluxionality of the nonmagic clusters (Pt_{11-13}) versus the magic Pt_{10} cluster is remarkably pronounced. For both the minimum and maximum interatomic distances, Pt_{10} has a much narrower spread, with the low-energy structures confined to minimum Pt−Pt distances of 2.52 to 2.54 Å and maximum Pt−Pt distances of 5.0 t o5.2 Å, whereas the other size clusters have a much larger spread and multiple points nearly intersecting the global minimum energy (the vertical lines) in Figure 4; this is especially pronounced for the maximum Pt−Pt distance, which shows a spread over 2 Å for Pt_{13}. Hence, the difference in structural diversity between the magic clusters and the fluxional nonmagic clusters becomes visually obvious.

Shape-Energy Correlation. To further differentiate the shapes of these clusters, we can look at η, a measure of the prolateness/oblateness of the cluster spheroid in Figure 5. Clusters that differ in η can be expected to be structurally inequivalent. We can clearly see that the low-lying isomers of Pt_{10} have very similar shapes close to the global minimum, with η close to zero and the spread in cluster shape sharply decreasing toward the vertical line at zero relative energy, whereas for $n = 11-13$, we can see points nearly intersecting the zero-relative-energy line at multiple points on the graph, sometimes with significantly with different η values. This is further evidence of the fluxionality of nonmagic Pt clusters (Pt_{11-13}) where there may exist many different structural conformations of a cluster with similarly low energies.

Structure Analysis of Pt_{12}. We take an in-depth look at the low-lying isomers by selecting the nonmagic Pt_{12} as a case study. Unlike Pt_{10}, Pt_{12} is an experimentally reactive cluster[8,31] whose fluxionality may explain the significantly different catalytic performance when compared with Pt_{10}. In Figure 6a, we can see multiple motifs with similarly low energies by selecting structures with different η (oblateness/prolateness). These different low-energy structures can be symmetric or

asymmetric and are structurally unique. In Figure 6b, we see that both structures with high and low average coordination number can be low in energy, but the lowest energy structure falls somewhere in between the two displayed structures. In Figure 6c, we look at the variance of the cluster, calculated as the variance of the atomic distance from the center of mass of the cluster. This descriptor can be understood as a combined effect of the minimum and maximum Pt−Pt distances shown in Figure 4. A high variance corresponds to a diffuse cluster with atoms spaced out from each other, whereas a low variance corresponds to a cluster whose atoms are very tightly bound, so variance offers a useful single value to describe the diffuseness of the structure. We see that lower energy clusters tend toward the lower variance structures, where the cluster is closer to the center of mass and is correspondingly less diffuse. However, we can also discern an "island" of stability as highlighted by Figure 6c(ii), where the structure is flatter and has a correspondingly higher variance but is only 0.21 eV higher in energy than the global minimum [Figure 6c(i)].

Implications. This work represents an in-depth investigation into the structure-energy relationships of subnanometer Pt clusters by taking advantage of the large number of basin-hopping local minima in the configuration space from DFT local minimization. In the study of metal clusters, especially ones that exhibit high degrees of fluxionality, it is often not sufficient to only study several putative global minima, but a much broader configurational region is needed to have a better view of the energy landscape. We found a high degree of fluxionality for the Pt_{11-13} clusters from the large spread in values of the structural descriptors of the sampled low-energy structures from bond distances to coordination to shape. This high degree of fluxionality may provide insights into the high catalytic activity of small Pt clusters for a variety of reactions. The high fluxionality and low symmetry of these clusters may allow for the better bonding and accommodation of adsorbates to the surface. This study also highlights the importance of sufficiently sampling the configuration space of low-energy structures for energetically relevant configurations that may still be structurally diverse instead of a single global minimum.

Pt_{10} is much less fluxional than the other sizes due to its magic nature. This is probably also true for Pd_{10} and Au_{10}, but not for Ag_{10}, because Ag_{10} has been found not to be a magic cluster,[37] while Au_{10} has a planar geometry.[38] The clear differences in fluxionality in the studied Pt clusters are a promising result toward the future investigation of larger cluster sizes, including the possible Pt magic clusters of $n = 14$ and 20, which have been prepared in a dendrimer recently.[10] While we have studied the thermodynamic stability of the global and low-lying minima for Pt clusters, the kinetics of the system are still relatively uncharacterized. Future work regarding the kinetics of cluster fluxionality can be carried out by mapping out transition states connecting different minima or using molecular dynamics to explore the atomistic processes of basin hopping under realistic temperatures.

4. CONCLUSIONS

Using DFT-based basin hopping for global minimization, we explored both the most stable structures and the structure diversity of Pt_n ($n = 10-13$) clusters. We confirmed that Pt_{10} is a magic cluster with a global minimum of tetrahedral geometry but found that the other clusters have less symmetric global minima. By analyzing all of the local-minimum structures from

the basin-hopping searches, we examined the relationships of coordination number, interatomic distances, and cluster shape versus cluster energy. While, in general, qualitative trends could be drawn from these relationships, we found a significant spread in these geometric quantities with respect to energy. In particular, many low-lying isomers could be found for Pt_{11-13} which are structurally distinct but energetically similar, suggesting a high degree of fluxionality for clusters of this size. This fluxionality could be important in catalysis by subnanometer Pt clusters.

■ ASSOCIATED CONTENT

Ⓢ Supporting Information

The Supporting Information is available free of charge on the ACS Publications website at DOI: 10.1021/acs.jpcc.6b11968.

Coordinates for the global minima of Pt_n ($n = 10-13$) clusters. (PDF)

■ AUTHOR INFORMATION

Corresponding Author

*E-mail: djiang@ucr.edu. Tel.: +1-951-827-4430.

ORCID Ⓞ

De-en Jiang: 0000-0001-5167-0731

Notes

The authors declare no competing financial interest.

■ REFERENCES

(1) Yamamoto, K.; Imaoka, T.; Chun, W. J.; Enoki, O.; Katoh, H.; Takenaga, M.; Sonoi, A. Size-Specific Catalytic Activity of Platinum Clusters Enhances Oxygen Reduction Reactions. *Nat. Chem.* **2009**, *1*, 397−402.

(2) Guo, S.; Zhang, S.; Sun, S. Tuning Nanoparticle Catalysis for the Oxygen Reduction Reaction. *Angew. Chem., Int. Ed.* **2013**, *52*, 8526−8544.

(3) Schweinberger, F. F.; Berr, M. J.; Döblinger, M.; Wolff, C.; Sanwald, K. E.; Crampton, A. S.; Ridge, C. J.; Jäckel, F.; Feldmann, J.; Tschurl, M.; et al. Cluster Size Effects in the Photocatalytic Hydrogen Evolution Reaction. *J. Am. Chem. Soc.* **2013**, *135*, 13262−13265.

(4) Nesselberger, M.; Roefzaad, M.; Hamou, R. F.; Biedermann, P. U.; Schweinberger, F. F.; Kunz, S.; Schloegl, K.; Wiberg, G. K.; Ashton, S.; Heiz, U.; et al. The Effect of Particle Proximity on the Oxygen Reduction Rate of Size-Selected Platinum Clusters. *Nat. Mater.* **2013**, *12*, 919−924.

(5) Vajda, S.; et al. Subnanometre Platinum Clusters as Highly Active and Selective Catalysts for the Oxidative Dehydrogenation of Propane. *Nat. Mater.* **2009**, *8*, 213−6.

(6) Tyo, E. C.; Vajda, S. Catalysis by Clusters with Precise Numbers of Atoms. *Nat. Nanotechnol.* **2015**, *10*, 577−588.

(7) Vajda, S.; White, M. G. Catalysis Applications of Size-Selected Cluster Deposition. *ACS Catal.* **2015**, *5*, 7152−7176.

(8) Imaoka, T.; Kitazawa, H.; Chun, W.-J.; Omura, S.; Albrecht, K.; Yamamoto, K. Magic Number Pt_{13} and Misshapen Pt_{12} Clusters: Which One Is the Better Catalyst? *J. Am. Chem. Soc.* **2013**, *135*, 13089−13095.

(9) Heiz, U.; Sanchez, A.; Abbet, S.; Schneider, W.-D. Catalytic Oxidation of Carbon Monoxide on Monodispersed Platinum Clusters: Each Atom Counts. *J. Am. Chem. Soc.* **1999**, *121*, 3214−3217.

(10) Imaoka, T.; Kitazawa, H.; Chun, W. J.; Yamamoto, K. Finding the Most Catalytically Active Platinum Clusters with Low Atomicity. *Angew. Chem., Int. Ed.* **2015**, *54*, 9810−9815.

(11) Calle-Vallejo, F.; Martínez, J. I.; García-Lastra, J. M.; Sautet, P.; Loffreda, D. Fast Prediction of Adsorption Properties for Platinum Nanocatalysts with Generalized Coordination Numbers. *Angew. Chem., Int. Ed.* **2014**, *53*, 8316−8319.

(12) Calle-Vallejo, F.; Tymoczko, J.; Colic, V.; Vu, Q. H.; Pohl, M. D.; Morgenstern, K.; Loffreda, D.; Sautet, P.; Schuhmann, W.; Bandarenka, A. S. Finding Optimal Surface Sites on Heterogeneous Catalysts by Counting Nearest Neighbors. *Science* **2015**, *350*, 185−189.

(13) Jiang, D.-e.; Walter, M. Au_{40}: A Large Tetrahedral Magic Cluster. *Phys. Rev. B: Condens. Matter Mater. Phys.* **2011**, *84*, 193402.

(14) Priest, C.; Tang, Q.; Jiang, D.-e. Structural Evolution of Tc_n (N= 4−20) Clusters from First-Principles Global Minimization. *J. Phys. Chem. A* **2015**, *119*, 8892−8897.

(15) Wales, D. J.; Doye, J. P. Global Optimization by Basin-Hopping and the Lowest Energy Structures of Lennard-Jones Clusters Containing up to 110 Atoms. *J. Phys. Chem. A* **1997**, *101*, 5111−5116.

(16) Watanabe, Y.; Wu, X.; Hirata, H.; Isomura, N. Size-Dependent Catalytic Activity and Geometries of Size-Selected Pt Clusters on TiO_2 (110) Surfaces. *Catal. Sci. Technol.* **2011**, *1*, 1490−1495.

(17) Nie, A.; Wu, J.; Zhou, C.; Yao, S.; Luo, C.; Forrey, R. C.; Cheng, H. Structural Evolution of Subnano Platinum Clusters. *Int. J. Quantum Chem.* **2007**, *107*, 219−224.

(18) Kumar, V.; Kawazoe, Y. Evolution of Atomic and Electronic Structure of Pt Clusters: Planar, Layered, Pyramidal, Cage, Cubic, and Octahedral Growth. *Phys. Rev. B: Condens. Matter Mater. Phys.* **2008**, *77*, 205418.

(19) Chaves, A. S.; Rondina, G. G.; Piotrowski, M. J.; Tereshchuk, P.; Da Silva, J. L. The Role of Charge States in the Atomic Structure of Cu_n and Pt_n (N= 2−14 Atoms) Clusters: A Dft Investigation. *J. Phys. Chem. A* **2014**, *118*, 10813−10821.

(20) Jiang, D. e.; Walter, M.; Dai, S. Gold Sulfide Nanoclusters: A Unique Core-in-Cage Structure. *Chem. - Eur. J.* **2010**, *16*, 4999−5003.

(21) Kresse, G.; Furthmuller, J. Efficient Iterative Schemes for Ab Initio Total-Energy Calculations Using a Plane-Wave Basis Set. *Phys. Rev. B: Condens. Matter Mater. Phys.* **1996**, *54*, 11169−11186.

(22) Kresse, G.; Furthmuller, J. Efficiency of Ab-Initio Total Energy Calculations for Metals and Semiconductors Using a Plane-Wave Basis Set. *Comput. Mater. Sci.* **1996**, *6*, 15−50.

(23) Perdew, J. P.; Burke, K.; Ernzerhof, M. Generalized Gradient Approximation Made Simple. *Phys. Rev. Lett.* **1996**, *77*, 3865.

(24) Kresse, G.; Joubert, D. From Ultrasoft Pseudopotentials to the Projector Augmented-Wave Method. *Phys. Rev. B: Condens. Matter Mater. Phys.* **1999**, *59*, 1758.

(25) Blöchl, P. E. Projector Augmented-Wave Method. *Phys. Rev. B: Condens. Matter Mater. Phys.* **1994**, *50*, 17953−17979.

(26) Rodríguez-Kessler, P.; Rodríguez-Domínguez, A. Size and Structure Effects of Pt_N (N= 12− 13) Clusters for the Oxygen Reduction Reaction: First-Principles Calculations. *J. Chem. Phys.* **2015**, *143*, 184312.

(27) Gupta, S. K.; Nappi, B. M.; Gingerich, K. A. Mass Spectrometric Study of the Stabilities of the Gaseous Molecules Diatomic Platinum and Platinum-Yttrium. *Inorg. Chem.* **1981**, *20*, 966−969.

(28) Cheng, J.; Fournier, R. Structural Optimization of Atomic Clusters by Tabu Search in Descriptor Space. *Theor. Chem. Acc.* **2004**, *112*, 7−15.

(29) Wales, D. J.; Doye, J. P. K., Dullweber, A.; Hodges, M. P.; Naumkin, F. Y.; Calvo, F.; Hernández-Rojas, J.; Middleton, T. F. The Cambridge Cluster Database. http://www-wales.ch.cam.ac.uk/CCD.html (accessed November 15, 2016).

(30) Adlhart, C.; Uggerud, E. Reactions of Platinum Clusters $Pt_n^±$, N= 1−21, with Ch_4: To React or Not to React. *Chem. Commun.* **2006**, 2581−2582.

(31) Trevor, D.; Cox, D.; Kaldor, A. Methane Activation on Unsupported Platinum Clusters. *J. Am. Chem. Soc.* **1990**, *112*, 3742–3749.

(32) Balteanu, I.; Balaj, O. P.; Beyer, M. K.; Bondybey, V. E. Reactions of Platinum Clusters 195 $Pt_n^{\pm}$, N= 1−24, with N_2O Studied with Isotopically Enriched Platinum. *Phys. Chem. Chem. Phys.* **2004**, *6*, 2910−2913.

(33) Piotrowski, M. J.; Piquini, P.; Da Silva, J. L. Density Functional Theory Investigation of 3 D, 4 D, and 5 D 13-Atom Metal Clusters. *Phys. Rev. B: Condens. Matter Mater. Phys.* **2010**, *81*, 155446.

(34) Chou, J.; Hsing, C.; Wei, C.; Cheng, C.; Chang, C. Ab Initio Random Structure Search for 13-Atom Clusters of Fcc Elements. *J. Phys.: Condens. Matter* **2013**, *25*, 125305.

(35) Bunău, O.; Bartolomé, J.; Bartolomé, F.; Garcia, L. Large Orbital Magnetic Moment in Pt_{13} Clusters. *J. Phys.: Condens. Matter* **2014**, *26*, 196006.

(36) Błoński, P.; Hafner, J. Magneto-Structural Properties and Magnetic Anisotropy of Small Transition-Metal Clusters: A First-Principles Study. *J. Phys.: Condens. Matter* **2011**, *23*, 136001.

(37) Pereiro, M.; Baldomir, D.; Arias, J. Unexpected Magnetism of Small Silver Clusters. *Phys. Rev. A: At., Mol., Opt. Phys.* **2007**, *75*, 063204.

(38) Häkkinen, H.; Yoon, B.; Landman, U.; Li, X.; Zhai, H.-J.; Wang, L.-S. On the Electronic and Atomic Structures of Small Au N-(N= 4−14) Clusters: A Photoelectron Spectroscopy and Density-Functional Study. *J. Phys. Chem. A* **2003**, *107*, 6168−6175.